Hindawi
Mathematical Problems in Engineering
Volume 2021, Article ID 9930182, 12 pages
https://doi.org/10.1155/2021/9930182

Research Article

Optimization of the Structural Parameters and the Teeth Shape of Slip in Drill Rig

Hua Zhang,[1] **Qianwei Zhu**,[1] **and Bin Gao**[2]

[1]*School of Mechanical Engineering, Nantong University, Nantong, Jiangsu 226019, China*
[2]*Wuxi Amman Engineering Machinery Co., Ltd., Wuxi, Jiangsu 214000, China*

Correspondence should be addressed to Hua Zhang; ntuzhh@ntu.edu.cn

Received 22 March 2021; Revised 13 April 2021; Accepted 26 April 2021; Published 7 May 2021

Academic Editor: Xiaodong Sun

In order to improve the performance of slip and reduce the extrusion damage of the drill pipe in the drill rig, the optimization of structural parameters and teeth shape of the slip while clamping the drill pipe had been researched in this article. On the macroscale, the structural parameters of the slip had been optimized with response surface method (RSM) and Multiobjective Genetic Algorithm (MOGA). The optimized result showed that the single weight of the slip had been reduced from 3.99 kg to 2.91 kg and the maximum deformation of the drill pipe was reduced from 3.75 mm on both sides to 2.56 mm on both sides. On the microscale, a mathematical model for the single slip teeth while clamping the drill pipe had been established to give a detailed description to calculate the equivalent coefficient of friction and provide the relationship between the frictional torque with the allowable compression strength. In addition, the finite element model that had been set up by ABAQUS was used to verify the mathematical model, and the comparison of results had shown the accuracy of the mathematical model of the slip teeth while clamping the drill pipe. According to the mathematical model of the slip teeth in the drill rig, while clamping the drill pipe, the optimal shape of the slip teeth in the drill rig was achieved under the following condition: the slope of the slip teeth θ is 60°, the top width of the slip teeth w_h is 1.5 mm, and the depth of the slip teeth clamping the drill pipe d is 0.5 mm. The equivalent coefficient of friction f_v can be increased from 1.73 to 2.06, and the optimal result f_v increases 11.3%.

1. Introduction

As a consequence of sustained interest in the development of underground space, tunnels played a more and more important role in human production activities and life. Hence, drill rigs had been widely used in various construction occasions because of the high automatic and working efficiency [1, 2].

In the recent years, with the rapid development of anchoring construction and engineering construction, the crushing of the drill pipe has occurred frequently due to the more and more heavy and complex dynamic loadings. To solve this problem, a lot of research studies had been carried to analyze on the phenomenon and position of drill pipe failure mainly from the following four aspects: surface irregularities [3–5], upset area [6, 7], corrosion pitting [8, 9], and threaded connections [10–12].

In order to avoid slip crushing, this study used the response surface method (RSM) and multiobjective optimization genetic algorithm (MOGA) to optimize the structure of the slip; in addition, this study also proposed a mathematical model to describe the interaction of the slip teeth and drill pipe in a drill rig. The physical model drill rig is shown in Figure 1. The clamp was the most important module of the drill rig. It was always fixed in front of the propulsive frame and used to load or unload the drill pipe. The slip is also a key part of the clamp; there is a protuberant teeth which is called the slip teeth on the surface of slip. Three-dimensional schematic of the slip and the slip teeth is shown in Figure 1.

On the macroscale, we expected to reduce the slip crushing by optimizing the structural parameters of slip in the drill rig but the optimization is a nonlinear problem. Thus, it is difficult to establish an accurate mathematical model to evaluate and optimize the performance. Thanks to the research on progress of optimization methods. In [13], a new multilevel optimization strategy for efficient multiobjective

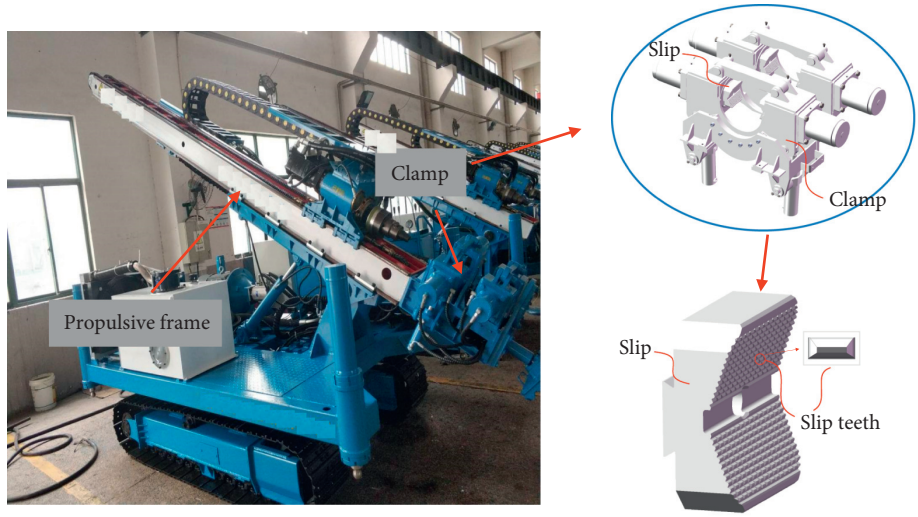

Figure 1: The installation location of the clamp and slip.

optimization was used for optimizing the design of interior permanent magnet synchronous motors (IPMSMs). Then, the Kriging model was employed to approximate the finite element analysis for the multiobjective optimization in each level. In [14], a novel multiobjective system level optimization method for SRM drive systems had been presented. A SRM drive system with a segmented-rotor switched reluctance motor (SSRM) and the angle position control method were investigated to verify the effectiveness of the proposed method. In addition, the optimization of structural parameters was another research hotspot [15, 16]. The design optimization research studies of the engineering machine had been developed rapidly. The most popular method for optimizing engineering machine was performed using finite element analysis (FEA) coupled with optimization algorithms such as genetic algorithm (GA) [17], multiobjective genetic algorithm [18,19], and nondominated sorting genetic algorithm-II (NSGA-II) [20, 21].

On the microscale, we wanted to establish a mathematical model for the single slip teeth, while clamping the drill pipe to reduce the slip crushing. The analysis of drill pipe failure due to the slip teeth could be traced back to the work by Reinhold and Spiri [22] in 1959. By regarding the slip system as an immoveable wedge, the ratio of the transverse loading to the axial loading can be derived and the average radial pressure acting on the outer wall of the drill pipe can be estimated. In this way, a formula for calculating the crushing load can be obtained by combining the axial stress and the tangential stress. Vreeland [23] verified the Reinhold–Spiri formula by carrying out eight groups of tests on 5 in drill pipes. The results had shown a satisfactorily fitting of the Reinhold–Spiri formula. Then, Hayatdavoudi [24] and Sathuvalli et al. [25] had performed research studies on reducing the probability of drill pipe yielding. Tang et al. [26] and Qian [27] used the FE model to study how the slip-insert geometry affects the mechanical behavior of the drill pipe.

This study work included the following three contents. Firstly, the structure of the slip could be optimized to reduce the deformation of the drill pipe by the method of RSM and MOGA. Secondly, the mathematical model was used to calculate the equivalent coefficient of friction and provide the relationship between the torque with the allowable compression strength. Finally, the mathematical model was verified by the finite element model which was established by ABAQUS, and the optimization parameters of the slip teeth had been presented.

2. Optimization of the Structure of the Slip by RSM and MOGA

2.1. Determination of Optimized Parameters and DOE Experiment Design. The slip is usually machined from a square piece by NC milling. There are four vertical sides at the top, bottom, left, and right. In front of the slip, there are two symmetrical slip teeth surfaces. The two slip teeth surfaces are at a certain angle with the horizontal direction. The specific structure is shown in Figure 2. As shown in Figure 2, the length and the width of the slip are represented by P_1 and P_2, respectively. The angle between the teeth surface and horizontal direction is represented by P_3. P_1, P_2, and P_3 are selected as the optimal design parameters.

According to the position between specific structures interference combined with design skills that include the diameter of the drill pipe, the size restriction of the roughneck guide device, and the width/ thickness ratio of the slip, the optimization range of design parameters could be concluded as shown in Table 1.

According to the optimization design object slip, slip mass (P_4) and drill pipe deformation (P_5) were taken as output parameters. Box Behnken Design (BBD) was used to design the experiment; meanwhile, the combination of design parameters was obtained to construct the response surface.

2.2. Establishment and Analysis of Standard Second-Order RSM. The standard regression equation was used to establish the mathematical model, which can be established as shown in the following equation:

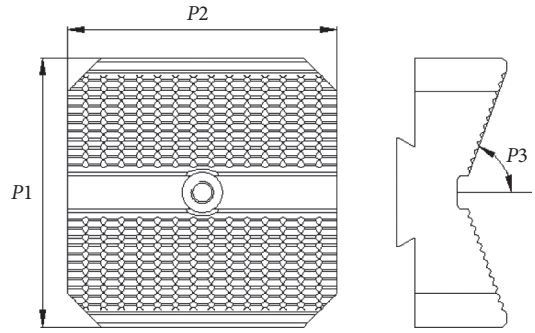

Figure 2: The diagram of the slip structure.

Table 1: Initial value and optimization range of design parameters.

Design parameters	Initial value	Optimization range of design parameters
P_1 (mm)	120	96 ~ 144
P_2 (mm)	120	96 ~ 144
P_3 (degree)	70	56 ~ 84

$$\hat{y} = a + \sum_{j=1}^{m} b_j x_j + \sum_{j=1}^{m} b_{jj} x_j^2 + \sum_{j<k} b_{jk} x_j x_k + \varepsilon, \quad (1)$$

where $\hat{y}$ is the regression prediction value of output parameters, x_j is, respectively, corresponding to the values of input parameter P_j, a is the constant coefficient value, b_j, b_{jj}, and b_{ij} are the coefficient values of the corresponding input parameter, and ε is the statistical error value. This is a FE simulation analysis, and the value of ε is taken as 0.

A model for the standard quadratic response surface was established based on all quadratic terms, primary terms, and the interaction between various factors. With the calculation of software, the regression mathematical model of slip mass and drill pipe deformation with three design parameters can be obtained:

$$\begin{aligned} \hat{y}_4 &= 1.61 + 0.07X_1 + 0.13X_2 + 0.14X_3 - 0.01X_1^2 + 0.005X_2^2 + 0.008X_3^2 + 0.002X_1X_2 + 0.04X_1X_3 + 0.005X_2X_3, \\ \hat{y}_5 &= 10.76 - 0.63X_2 + 10.17X_3 + 0.01X_1^2 + 3.57X_3^2 + 0.21X_1X_3, \end{aligned} \quad (2)$$

where $\hat{y}_4$ and $\hat{y}_5$ are, respectively, regression prediction values of the parameter of slip mass and drill pipe deformation and X_1, X_2, and X_3 are, respectively, corresponding to input parameters P_1, P_2, and P_3 after Yeo–Johnson transformation [28].

The output results of P_4 and P_5 from RSM and the design parameters P_1, P_2, and P_3 are shown in Figure 3. When the length of the slip is between 100–110 mm, the drill pipe deformation will have a great drop and then gradually becomes stable, as shown in Figure 3(a). It can be seen from Figure 3(b) that the deformation of the drill pipe decreases with the increase of the width of the slip. When the slip surfaces' angle is about 60°, the drill pipe deformation achieves the minimum value within the optimized range, as shown in Figure 3(c).

2.3. The Multiobjective Optimization Model of the Slip Structure. By establishing the mathematical regression model of output parameters, the method of MOGA was used to optimize the structural parameters of the slip. The optimization constraints were set as the minimum slip mass and the minimum deformation of drill pipe while clamping; the upper limit value of design variable $\overline{x} = [144, 144, 70]^T$ and the lower limit value of design variable $\underline{x} = [96, 96, 56]^T$.

Table 2 had shown the eight Pareto optimal solutions obtained by importing software for MOGA calculation. According to the results given in Table 2, the optimal solution of width of the slip and the surface angle of the slip has a steady trend around a fixed value besides the length of slip changes in a large range. These observations implied that, with the increase of the length of the slip, although the mass of the slip was slightly increased, there was a significant decrease in the deformation of the drill pipe.

By analyzing the eight optimization results listed in Table 2 and combining with the processing technology at the same time, three groups of MOGA calculations were round-up. The final optimized results are shown in Table 3.

Considering the main optimization object as the deformation of the drill pipe, the third group was preferred. Under the same working circumstance, the single weight of the slip is reduced from 3.99 kg to 2.91 kg and the maximum deformation of the drill pipe is reduced from 3.75 mm on both sides to 2.56 mm on both sides.

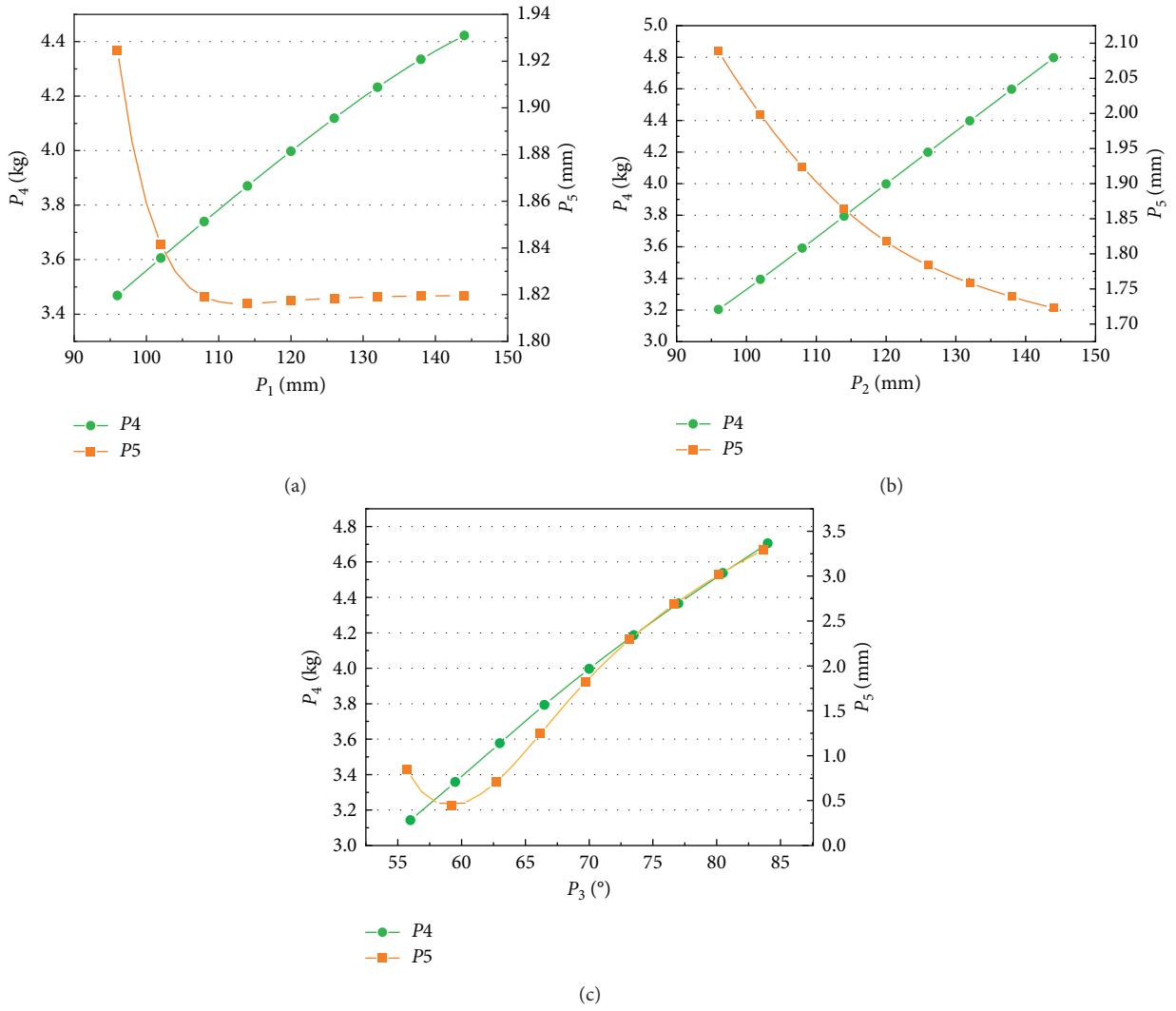

Figure 3: Output results of P_4 and P_5 by the response surface method. (a) Output results with different lengths of the slip. (b) Output results with different widths of the slip. (c) Output results with different slip angles.

Table 2: Eight groups of optimal solutions under the MOGA calculation.

	P_1 (mm)	P_2 (mm)	P_3 (°)
First group	111.87	97.32	59.05
Second group	120.73	99.44	58.53
Third group	130.8	97.13	59.04
Forth group	123.28	99.6	59.02
Fifth group	130.65	97.39	59.22
Sixth group	130.67	97.46	59.23
Seventh group	130.67	97.46	59.23
Eighth group	130.32	97.44	59.25

Table 3: Three groups of the most optimal calculations.

	First group	Second group	Third group
P_1 (mm)	110	120	130
P_2 (mm)	100	100	100
P_3 (°)	60	60	60
P_4 (kg)	2.76	2.84	2.91
P_5 (mm)	1.31	1.31	1.28

3. Mathematical Model of Conclusion for the Slip Teeth and Drill Pipe

3.1. Special Considerations. Considering the complex phenomenon of the multiple slip teeth clamp drill pipe at the same time, the following hypotheses [29, 30] were made before the governing equations had been given:

(1) Considering only one slip teeth clamps the drill pipe

(2) The slip teeth is a rigid body

(3) The drill pipe is a linear elastic deformable body

3.2. The Antislide Model. Figure 4 shows the model of the single-slip teeth clamp drill pipe. In the model, the slip teeth is clamping into the drill pipe under the pressure of hydraulic pressure. To make it easy to explain the mathematical model, the slip teeth in Figure 4 scaled five times.

As shown in Figure 4, the tangential force of the slip teeth can be stated as

$$F_c = \frac{T}{R-d}, \tag{3}$$

where T is the drill pipe torque, F_c is the tangential force caused by torque moment, R is the outer radius of the drill pipe, and d is the depth of the slip teeth clamping into the drill pipe.

Considering that the torque moment always squeezes the one side of the slip teeth, the squeeze side will achieve great frictional force, respectively. The friction force can be obtained by orthogonal decomposing of the tangential force (*Fc*) caused by torque moment.

As shown in Figure 4, the friction force can be stated as

$$F_f = F_n \cdot f, \tag{4}$$

where f is the coefficient of friction between the slip teeth and drill pipe, F_f is the friction force, and F_n is the normal component of the tangential force caused by torque moment. The pressing force can be described as

$$F_n = F_c \cos \angle OAB. \tag{5}$$

According to the angle relationship in ΔOAB, the $\angle OAB$ and $\overline{OB}$ can, respectively, be calculated as follows:

$$\overline{OB} = R - d - \frac{w_h}{2}\cot\theta, \tag{6}$$

$$\frac{R}{\sin\angle OBA} = \frac{\overline{OB}}{\sin\angle OAB}, \tag{7}$$

$$\sin\angle OAB = \frac{R-d-(w_h/2)\cot\theta}{R}\sin\theta, \tag{8}$$

where w_h is the top width of the slip teeth and θ is the slope of the slip teeth.

Substituting (8) into (5), it can be expressed as

$$F_n = F_c\sqrt{1-\left(\frac{R-d-(w_h/2)\cot\theta}{R}\sin\theta\right)^2}. \tag{9}$$

Considering that the slip teeth is acting slowly while working, the force balance formula can be expressed as static analysis:

$$F_t = F_f\cos\theta + F_n\sin\angle OAB, \tag{10}$$

$$F_n\cos\angle OAB = F_f\sin\theta, \tag{11}$$

where F_t is the total force of preventing the slide between the slip teeth and the drill pipe:

$$F_t(R-d)f_v = T. \tag{12}$$

According to the above equation, the result of the antislide model can be calculated as

$$F_t \geq \frac{T}{(R-d)f_v}. \tag{13}$$

The slip teeth and the drill pipe are not allowing to slide each other. Therefore, the equivalent friction torque generated when the slip teeth is stuck into the outer wall of the drill pipe should be greater than the resistance torque, and it can be expressed as

$$f_v = \frac{1}{f\cos\theta\sqrt{1-(((R-d-(w_h/2)\cot\theta)/R)\sin\theta)^2} + ((R-d-(w_h/2)\cot\theta)/R)\sin\theta\sqrt{1-(((R-d-(w_h/2)\cot\theta)/R)\sin\theta)^2}}, \tag{14}$$

where f_v is the equivalent coefficient of friction between the slip teeth and the drill pipe.

Once slip occurs between the slip teeth and the outer wall of the drill pipe, both the slip teeth and the drill pipe will be broken fast. If the resistance torque does not fit the relationships in equation (11), it will not only affect the normal working state of the slip teeth but also accelerate the rate of breaking of both the slip teeth and drill pipe.

3.3. The Compressive Stress Model. Considering that the compressive stress needs to be calculated, the area of the vertical component of tangential force caused by torque moment must be provided. According to equation (10), the normal component of the tangential force caused by torque moment F_n has been calculated.

As shown in Figure 4, the area of the vertical component of tangential force caused by torque moment can be expressed as

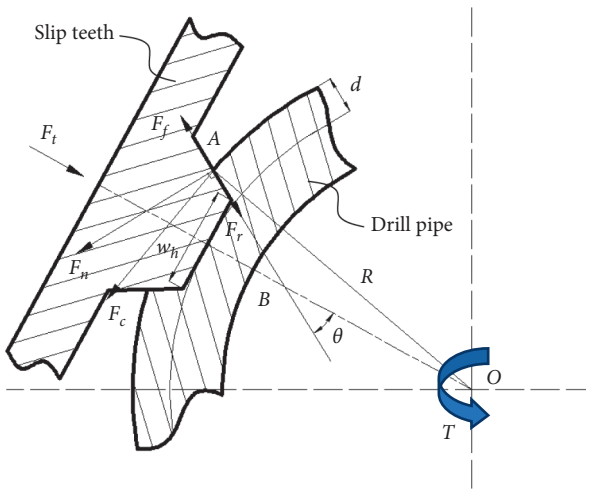

Figure 4: The model of the single-slip teeth clamping into the drill pipe.

$$A_n = lt \sec\frac{\theta}{2}. \tag{15}$$

Combining equation (9) with (15), the compression stress of the drill pipe can be expressed as

$$\sigma_n = \frac{T\sqrt{1-\left(\left((R-d-(w_h/2)\cot\theta)/R\right)\sin\theta\right)^2}}{(R-d)lt\sec(\theta/2)}. \tag{16}$$

In the above formula, equation (13) can also be expressed as inequality:

$$T \le \frac{(R-d)lt\sec(\theta/2)}{\sqrt{1-\left((R-d-(w_h/2)\cot\theta/R)\sin\theta\right)^2}}[\sigma_n], \tag{17}$$

where $[\sigma_n]$ is the allowable compression strength of the drill pipe. If the drill pipe torque is more than the allowable compression strength of the drill pipe, the drill pipe will undergo plastic deformation. Since the plastic deformation cannot resume, the plastic deformation of the drill pipe must be avoided.

4. The Finite Element Model Verification

4.1. The Establishment of the Finite Element Model. The model of the slip teeth and the drill pipe is shown in Figure 5. R_1 and R_2 are the external diameter and the inner diameter of the drill pipe; θ, ζ, and w_h, respectively, are the thread angle, the height of the slip teeth, and the top width of the slip teeth; d is clamp depth. The values are shown in Table 4.

Considering that the strain of the drill pipe must be controlled in the elastic scope, the material of the drill pipe can be given a general property of the linear elastic steel which has density of 7.85e-9 ton/mm^3, Young's modulus of 2.1e5 MPa, and Poisson's ratio of 0.3.

The model of the slip teeth clamping the drill pipe can be substituted as the 2D model, as shown in Figure 6(a). The finite element analysis of the 2D model of the slip teeth and the drill pipe was implemented by using the finite element analysis ABAQUS software. The pinball of the mesh where the slip teeth clamping the drill pipe should be more fine for the accurate results is shown in Figure 6(b). The elements' type of the drill pipe is CPS4R which has 4 nodes and 1 Gauss point; the number of elements of the drill pipe is 1168.

The contact between the slip teeth and the drill pipe can be set as surface-to-surface contact. The surface of the slip teeth is the master surface, and the surface of the drill pipe is the slave surface.

4.2. The Boundary and Solver Control of the Finite Element Model. The boundary of the finite element model is shown in Figure 7. As shown in Figure 7, the edge A is the inner boundary of the drill pipe. Reference A is the circle center of the drill pipe. Reference B is the middle point of the slip teeth.

There are two solver steps in this analysis. In the first solver step, the edge A is coupling to reference point A and the slip teeth is coupling to the reference point B; then, the fixed constraint in x and y directions is applied on reference point A, and 2 mm displacement at y direction is applied on reference point B. In the second solver step, 30,000 N/mm torque in rotation z is applied on reference point A and the boundary of the reference point B is preserved.

Under the great torque, the deformation of the drill pipe is so large that the elements have great change in FEM analysis. Therefore, the quasi-static [31] analysis by the explicit solver should be used to substitute to the implicit analysis by the standard solver.

4.3. The Verification of the Finite Element Model. According to equations (3) and (6), the normal component of the tangential force caused by torque moment can be calculated:

$$F_n = \frac{T}{R-d}\sqrt{1-\left(\frac{R-d-(w_h/2)\cot\theta}{R}\sin\theta\right)^2}. \tag{18}$$

Based on the parameters of Table 4 and 30,000 N/mm torque, F_n can be calculated by equation (18).

To get the reaction force normal component of the tangential force caused by torque moment, the reaction force of nodes at the boundary must be all counted. As shown in Figure 8, the master surface is the boundary of the teeth clamp with the solid edge and the slave surface is the boundary of the drill pipe with the dash edge. The contact area is between the solid edge with the dash edge. The nodes from N1 to N13 are the nodes of the slip teeth during the contact area. The value of the node force at the contact surface can be extracted by ABAQUS, and the reaction force caused by torque moment is equal to the sum of the node force at the contact surface.

As shown in figures 9(a)–9(c), the value of F_n which, respectively, calculated by the finite element model and mathematical model had been compared under the different parameters of d, w_h, and θ.

According to figures 9(a)–9(c), the tangential force caused by torque moment F_n can also be extracted by the

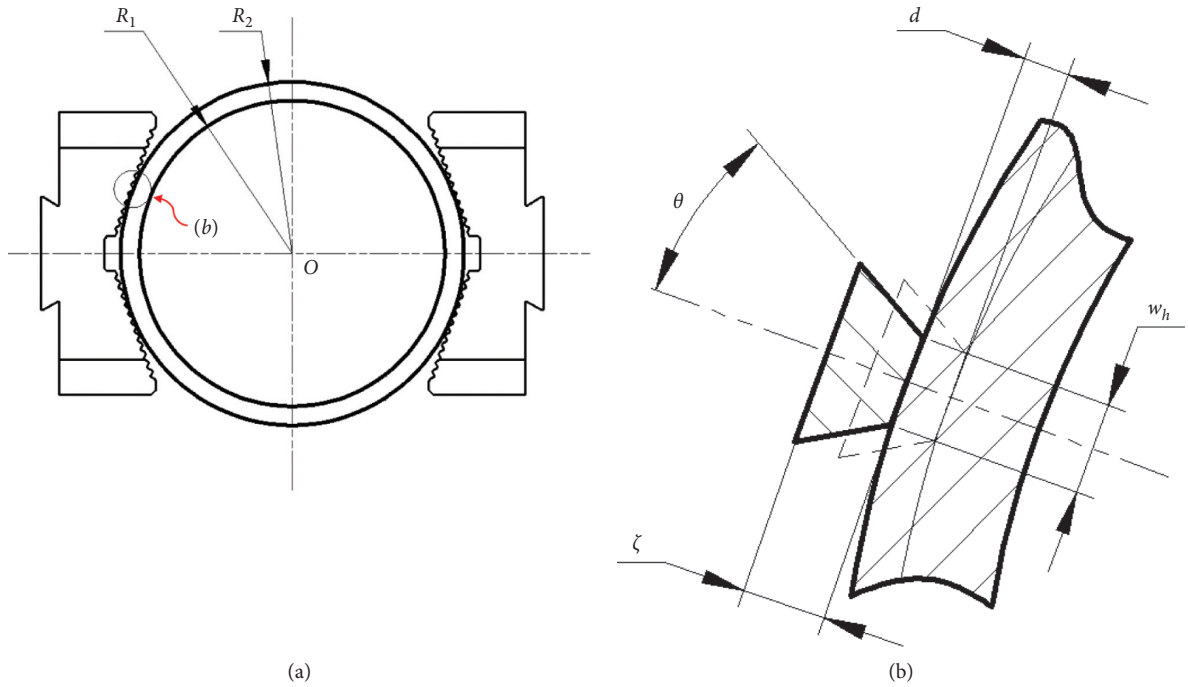

Figure 5: Diagram of the model of the slip teeth and drill pipe. (a) Diagram of the model of the drill pipe. (b) Diagram of the model of the slip teeth.

Table 4: The parameters of the slip teeth and the drill pipe.

Parameters	Value
R_1 (mm)	65
R_2 (mm)	73
Θ (°)	30°
ζ (mm)	2
w_h (mm)	2
d (mm)	1

finite element model. By comparing the result of the mathematical model with the result of the finite element model, the result of the mathematical model is all close to the result of the finite element model. It proves that the mathematical model can get a good confirmation to the finite element model.

5. The Optimization and Analysis of the Slip Teeth

According to equation (14), the depth of the slip teeth clamping the drill pipe d, the top width of the slip teeth w_h, and the slope of the slip teeth θ had been chosen as the key parameters. The equivalent coefficient of friction between the slip teeth and the drill pipe f_v had been chosen as the optimized target. The boundary constraint of design variables for the slip teeth structure can be set, as shown in Table 5.

According to the established mathematical model and combining the upper and lower limits of design variables, the different parameters about the trend chart of the equivalent coefficient of friction are shown in Figure 10. As shown in Figure 10(a), it is apparent that the slope of the slip teeth θ has large influence on the equivalent coefficient of friction f_v. When the slope of the slip teeth θ is set as 45°, the equivalent coefficient of friction f_v can achieve the minimum value. As shown in Figures 10(b) and 10(c), the depth of the clamp teeth clamping the drill pipe d and the top width of the clamp teeth w_h are nearly having no influence on the equivalent coefficient of friction f_v. According to Figure 10, it is obviously shown that f_v. is mainly related to θ; in addition, f_v has little relationship with other two parameters separately and interaction between two parameters.

The optimization parameters of slip teeth are set as follows: the slope of slip teeth θ is 60°, the top width of slip teeth w_h is 1.5 mm, and the depth of slip teeth d is 0.75 mm. As shown in Figure 10, the parameters of θ and w_h have nearly no influence on f_v; then, the values of parameters which are convenient for machining are preferred. The top width of the slip teeth w_h is chosen as 1.5 mm and the depth of slip teeth d is chosen as 0.75 mm, respectively. Under this circumstance, the equivalent coefficient of friction f_v can be increased from 1.73 to 2.06, and the optimal result f_v increases by 11.3%.

In the previous studies [30], Wei had optimized the slope of the triangle slip teeth θ by the orthogonal optimization method. Comparing the type of slip teeth in this research, the optimized result of the slope of triangle slip teeth θ was 55° ,which is similarity to 60°. By analyzing different profiles between the two slip teeth, the slip teeth in this research is a trapezoid slip tooth, while the slip teeth in the research of Wei's study was a triangle slip teeth with a filleted corner at the top of the triangle slip teeth. For the above mentioned

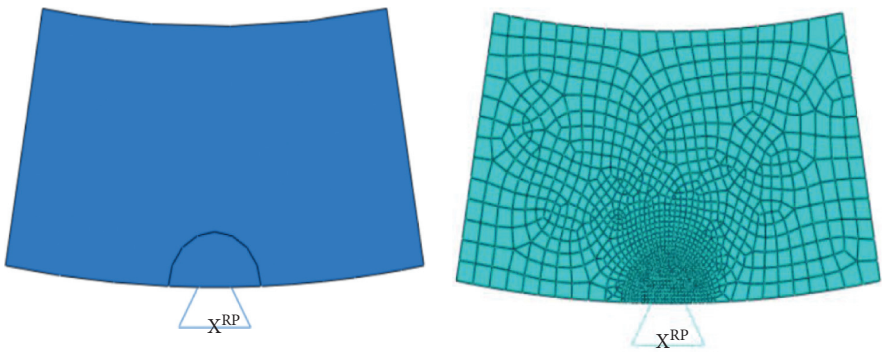

Figure 6: Finite element model of the slip teeth and the drill pipe. (a) Plane model. (b) Grid model.

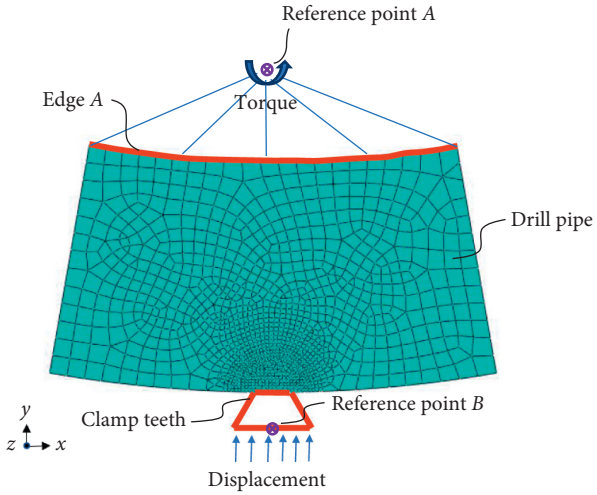

Figure 7: The boundary of the finite element model.

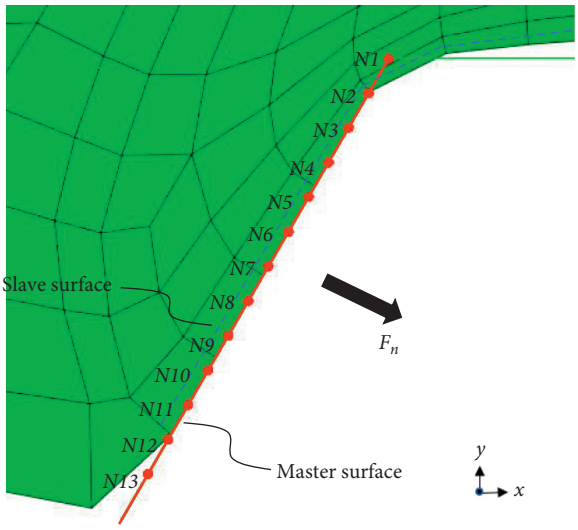

Figure 8: Diagram of the contact node area of the slip teeth and the drill pipe.

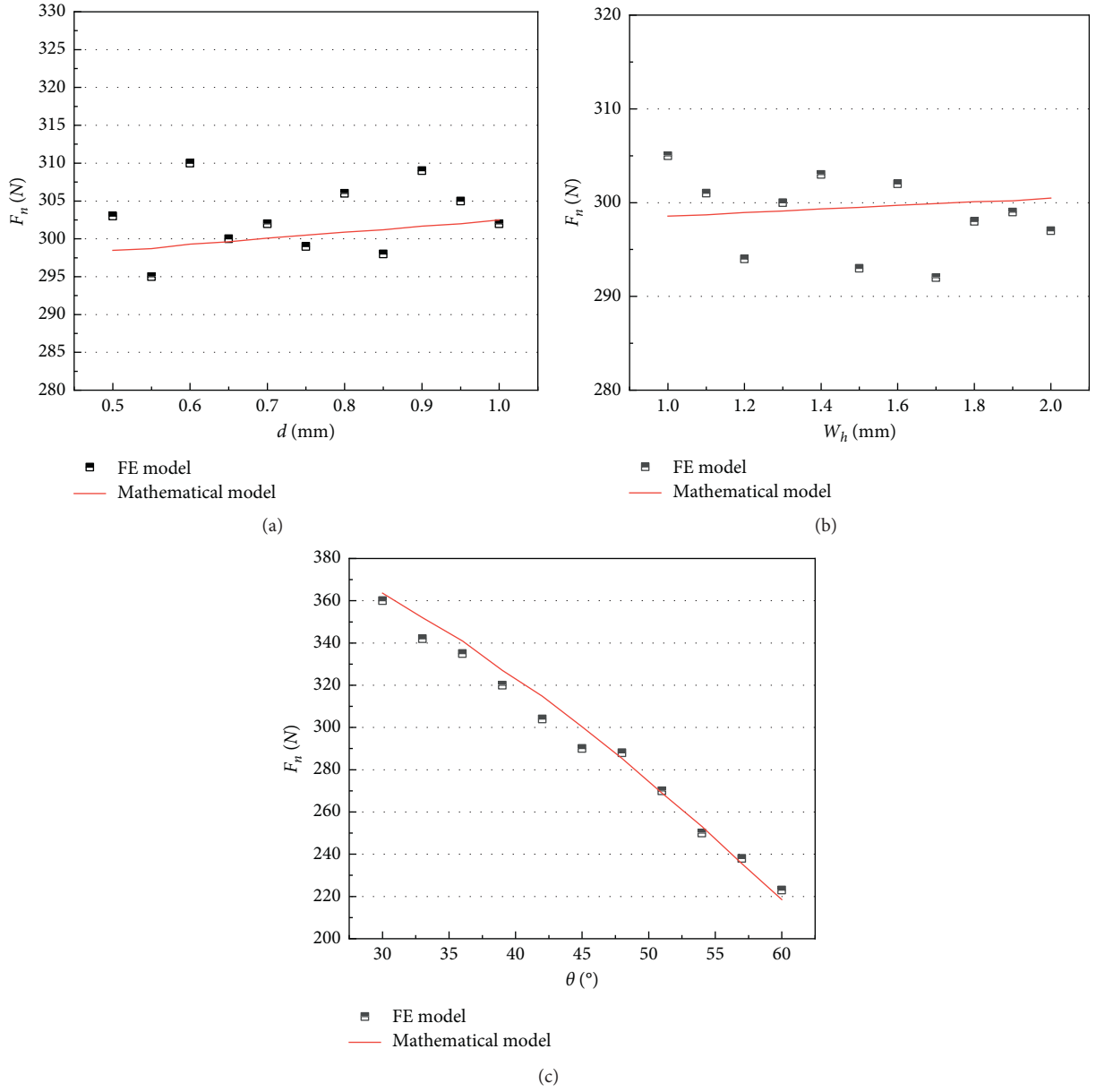

Figure 9: The FE model compared with the mathematical model under different parameters. (a) The normal component of the tangential force caused by torque moment F_n about d. (b) The normal component of the tangential force caused by torque moment F_n about w_h. (c) The normal component of the tangential force caused by torque moment F_n about θ.

Table 5: The boundary constraint of design variables for the slip teeth structure.

Design variables	Initial value	Variable range
d (mm)	0.75	(0.5, 1)
w_h (mm)	1.5	(1, 2)
θ (°)	45	(30, 60)

two types of the slip teeth, the optimization results had both shown that the slope of the slip teeth θ had achieved the upper of the optimization value. On the one hand, this phenomenon shows that the equivalent friction coefficient f_v has little effect on the profile shape of the slip teeth. On the other hand, it also shows that the larger the slope of the slip teeth θ is, the larger the theoretical equivalent friction coefficient is. Moreover, the comparison between the two types of slip teeth can also prove the accuracy of the established mathematical model in this study.

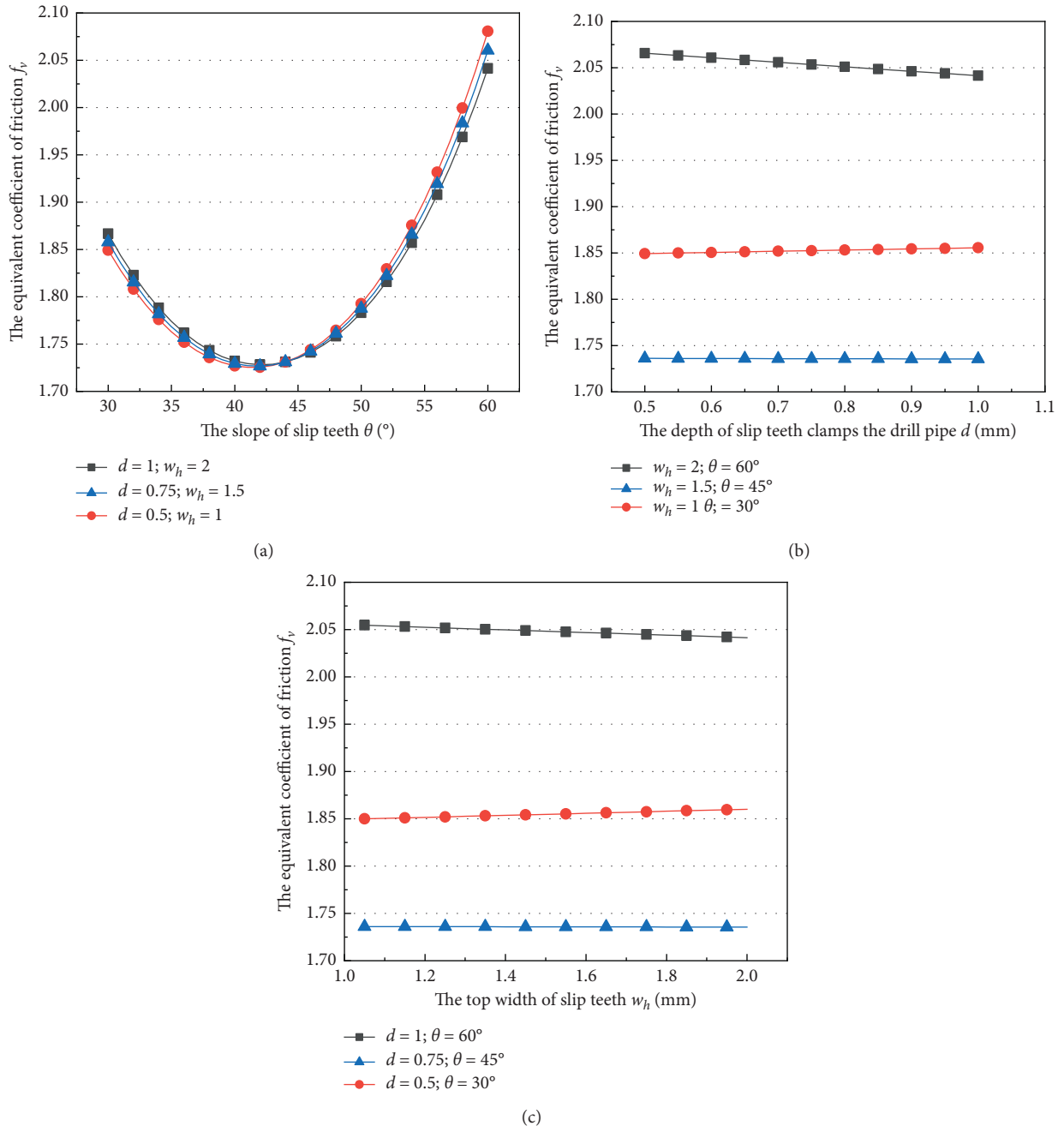

FIGURE 10: Different parameters about the trend chart of the equivalent coefficient of friction. (a) The trend chart about θ with f_v. (b) The trend chart about w_h with f_v. (c) The trend chart about d with f_v.

6. Conclusions

In this study, in order to prevent drill pipe damage because of slip, the optimization works include two contents. On the macroscale, the structural parameters of the slip had been optimized with RSM and MOGA. On the microscale, a mathematical model for the single-slip teeth clamping the drill pipe was established, and a finite element model was set up by ABAQUS to verify the mathematical model.

The following are the key conclusions drawn from this study.

(1) By the optimization of the slip based on the method of RSM, it is apparently shown that when the slip length $P1$ reaches 110 mm, the minimum deformation of the drill pipe is obtained; then, the minimum value does not decrease again as $P1$ increases. The deformation of the drill pipe is steadily decreasing as the slip width $P2$ increases. When the slip surfaces' angle is about 60°, the drill pipe deformation achieves the minimum value. With the method of MOGA, the optimal values can be calculated as $P1$ is 130 mm, $P2$ is 100 mm, and $P3$ is 60°. The weight of

the single slip had been reduced from 3.99 kg to 2.91 kg with a reduction rate of 27%, and the maximum deformation of the drill pipe had been reduced from 3.75 mm on both sides to 2.56 mm with a reduction of 31.9%.

(2) By simplifying the complex phenomenon of the multiple slip teeth clamp drill pipe at the same time, this study derived the mathematical model of the single-slip teeth clamp drill pipe. The equivalent coefficient of friction between the slip teeth and the drill pipe f_v could be set a relationship with the top width of the slip teeth w_h, the slope of the slip teeth θ, and the depth of the slip teeth clamping into the drill pipe d.

(3) The mathematical model was verified by the finite element model established by ABAQUS by extracting the value of the node force at the contact surface. Then, the FE model has a good fitting with the mathematical model of the single-slip teeth clamp drill pipe.

(4) The optimization parameters of the slip teeth had been given by analyzing the mathematical model. Through the single-factor comparison and cross-factor analysis between the three parameters, it was apparently shown that the slope of the slip teeth θ was taken as the primary factor. When the slope of the slip teeth θ was 60°, the top of slip teeth's width w_h was 1.5 mm and the depth of the slip teeth while clamping the drill pipe d was 0.5 mm. The equivalent coefficient of friction f_v could be increased from 1.73 to 2.06, and the optimal result f_v increased by 11.3%.

(5) Besides the optimization of the slip and slip teeth parameters, the topological shape of the slip and slip teeth will be the hot topic in the future research.

Data Availability

The data used to support the findings of this study are available from the corresponding author upon request.

Conflicts of Interest

The authors declare that there are no conflicts of interest regarding the publication of this paper.

Acknowledgments

The work was supported by the project funded by the Priority Academic Program Development of Jiangsu Higher Education Institutions and Science and Technology Development Fund Project of Wuxi.

References

[1] L. Zhao and M. Roh, "A thrust allocation method for efficient dynamic positioning of a semisubmersible drilling rig based on the hybrid optimization algorithm," *Mathematical Problems in Engineering*, vol. 2015, Article ID 183705, 12 pages, 2015.

[2] Q. Wang, H. Gao, B. Jiang et al., "Relationship model for the drilling parameters from a digital drilling rig versus the rock mechanical parameters and its application," *Arabian Journal of Geosciences*, vol. 11, pp. 357–370, 2018.

[3] C. Y. Jin, F. Qian, and F. P. Feng, "Effect of variable drill pipe sizes on casing wear collapse strength," *Journal of Petroleum Science and Engineering*, vol. 195, Article ID 107856, 2020.

[4] N. Lukin, R. T. Mouram, M. Alves et al., "Analysis of API S-135 steel drill pipe cutting process by blowout preventer," *Journal of Petroleum Science and Engineering*, vol. 195, Article ID 107819, 2020.

[5] N. H. Dao and H. Sellami, "Stress intensity factors and fatigue growth of a surface crack in a drill pipe during rotary drilling operation," *Engineering Fracture Mechanics*, vol. 96, no. 12, pp. 626–640, 2012.

[6] H. Zhu, Y. Lin, D. Zeng, Y. Zhou, and J. Xie, "Simulation analysis of flow field and shear stress distribution in internal upset transition zone of drill pipe," *Engineering Failure Analysis*, vol. 21, no. 4, pp. 67–77, 2012.

[7] Y. G. Liu, F. P. Li, X. Xu et al., "Simulation technology in failure analysis of drill pipe," *Procedia Engineering*, vol. 12, pp. 236–241, 2011.

[8] S. Lu, Y. Feng, F. Luo et al., "Failure analysis of IEU drill pipe wash out," *Fatigue*, vol. 27, no. 10, pp. 169–186, 2005.

[9] L. Han, M. Liu, S. Luo, and T. J. Lu, "Fatigue and corrosion fatigue behaviors of G105 and S135 high-strength drill pipe steels in air and H_2S environment," *Process Safety and Environmental Protection*, vol. 124, no. 4, pp. 63–74, 2019.

[10] S. Luo and S. Wu, "Effect of stress distribution on the tool joint failure of internal and external upset drill pipes," *Materials & Design (1980-2015)*, vol. 52, no. 12, pp. 308–314, 2013.

[11] Y. G. Li, F. P. Li, D. P. Yang et al., "Simulation on stress distribution of drill pipe's surface initial crack," *Applied Mechanics and Materials*, vol. 184, pp. 460–464, 2012.

[12] A. Baryshnikov, A. Calderoni, A. Ligrone, and P. Ferrara, "A new approach to the analysis of drillstring fatigue behaviour," *SPE Drilling & Completion*, vol. 12, no. 02, pp. 77–84, 1997.

[13] K. K. Diao, X. D. Sun, G. Lei et al., "Multi-objective design optimization of an IPMSM based on multi-level strategy," *IEEE Transactions on Industrial Electronics*, vol. 68, 2021.

[14] S. Luo and S. Wu, "Multiobjective system level optimization method for switched reluctance motor drive systems using finite element model," *IEEE Transactions on Industrial Electronics*, vol. 67, 2020.

[15] X. D. Sun, S. Zhou, J. G. Zhu et al., "Multi-objective design optimization of an IPMSM for EVs based on fuzzy method and sequential taguchi method," *IEEE Transactions on Industrial Electronics*, vol. 65, 2020.

[16] S. Zhou, X. D. Sun, Y. F. Cai et al., "Robust design optimization of a five-phase PM hub motor for fault-tolerant operation based on taguchi method," *IEEE Transactions on Industrial Electronics*, vol. 35, 2020.

[17] R. P. Brian and N. Mahmoudian, "Simulation-driven optimization of underwater docking station design," *IEEE Journal of Oceanic Engineering*, vol. 45, 2020.

[18] X. Fu, L. Lei, G. Yang, and B. Li, "Multi-objective shape optimization of autonomous underwater glider based on fast elitist non-dominated sorting genetic algorithm," *Ocean Engineering*, vol. 157, no. 3, pp. 339–349, 2018.

[19] M. L. Liao, Y. C. Zhou, Y. N. Su et al., "Dynamic analysis and multi-objective optimization of an offshore drilling tube system with pipe-in-pipe structure," *Applied Ocean Research*, vol. 75, no. 3, pp. 85–98, 2018.

[20] R. F. Huang, X. W. Luo, B. Ji et al., "Multi-objective optimization of a mixed-flow pump impeller using modified NSGA-II Algorithm," *Science China Technological Sciences*, vol. 58, no. 12, pp. 2122–2130, 2015.

[21] M. V. O. Camara, G. M. Ribeiro, C. R. Tosta et al., "A pareto optimal study for the multi-objective oil platform location problem with NSGA-II," *Journal of Petroleum Science and Engineering*, vol. 169, no. 5, pp. 258–268, 2018.

[22] W. B. Reinhold and W. H. Spiri, "Why does drill pipe fail in the slip area?" *World Oil*, vol. 100, pp. 10–20, 1959.

[23] J. T. Vreeland, "Deformation of drill pipe held in rotary slips," in *Proceedings Of the Petroleum Mechanical Engineering Conference*, Kansas City, MI, USA, September 1961.

[24] A. Hayatdavoudi, "Elastic yield of casing due to elevator/spider system," in *Proceedings Of the IADC/SPE Drilling Conference*, New Orleans, LA, USA, March 1985.

[25] U. B. Sathuvalli, M. L. Payne, P. V. Suryanarayana et al., "Advanced slip crushing considerations for deep-water drilling," in *Proceedings Of IADC/SPE Drilling Conference*, Dallas, TX, USA, February 2002.

[26] L. P. Tang, X. H. Zhu, J. H. Li, and C.-S. Shi, "Optimization analysis on the effects of slip insert design on drill pipe damage," *Journal of Failure Analysis and Prevention*, vol. 16, no. 3, pp. 384–390, 2016.

[27] X. D. Qian, "Failure assessment diagrams for circular hollow section X- and K-joints," *International Journal of Pressure Vessels and Piping*, vol. 104, pp. 43–56, 2013.

[28] R. A. Johnson and J. P. Klein, "6 Regression models for survival data," *Handbook of Statistics*, vol. 18, pp. 161–191, 2000.

[29] L. T. Guo, *"Mechanism Design of Iron Roughneck Torque Wrench and Mechanical Analysis of Pipe String Holder*, M.S. thesis, Xi'an Shiyou University, Xi an, China, 2019.

[30] L. Wei, *The Key Parameters of Iron Roughneck's Tong Dies Optimization Design*, M.S. thesis, Xi'an Shiyou University, Xi an, China, 2014.

[31] R. Jean Boulbes, *Troubleshooting Finite-Element Modeling with Abaqus with Application in Structural Engineering Analysis*, Springer Nature Switzerland AG, Berlin, Germany, 2020.